JOURNAL OF VIROLOGY, Dec. 2002, p. 12211–12222 Vol. 76, No. 23
0022-538X/02/$04.00+0 DOI: 10.1128/JVI.76.23.12211–12222.2002

The Hydrophilic Amino-Terminal Arm of Reovirus Core Shell Protein λ1 Is Dispensable for Particle Assembly

Jonghwa Kim,[1,2] Xing Zhang,[3] Victoria E. Centonze,[4]† Valorie D. Bowman,[3] Simon Noble,[2]‡ Timothy S. Baker,[4] and Max L. Nibert[1]*

Department of Microbiology and Molecular Genetics, Harvard Medical School, Boston, Massachusetts 02115[1]; Department of Biochemistry[2] and Integrated Microscopy Resource,[4] University of Wisconsin—Madison, Madison, Wisconsin 53706; and Department of Biological Sciences, Purdue University, West Lafayette, Indiana 47907[3]

Received 10 April 2002/Accepted 6 August 2002

The reovirus core particle is a molecular machine that mediates synthesis, capping, and export of the viral plus strand RNA transcripts. Its assembly and structure-function relationships remain to be well understood. Following the lead of previous studies with other *Reoviridae* family members, most notably orbiviruses and rotaviruses, we used recombinant baculoviruses to coexpress reovirus core proteins λ1, λ2, and σ2 in insect cells. The resulting core-like particles (CLPs) were purified and characterized. They were found to be similar to cores with regard to their sizes, morphologies, and protein compositions. Like cores, they could also be coated in vitro with the two major outer-capsid proteins, μ1 and σ3, to produce virion-like particles. Coexpression of core shell protein λ1 and core nodule protein σ2 was sufficient to yield CLPs that could withstand purification, whereas expression of λ1 alone was not, indicating a required role for σ2 as a previous study also suggested. In addition, CLPs that lacked λ2 (formed from λ1 and σ2 only) could not be coated with μ1 and σ3, indicating a required role for λ2 in the assembly of these outer-capsid proteins into particles. To extend the use of this system for understanding the core and its assembly, we addressed the hypothesis that the hydrophilic amino-terminal region of λ1, which adopts an extended arm-like conformation around each threefold axis in the reovirus core crystal structure, plays an important role in assembling the core shell. Using a series of λ1 deletion mutants, we showed that the amino-terminal 230 residues of λ1, including its zinc finger, are dispensable for CLP assembly. Residues in the 231-to-259 region of λ1, however, were required. The core crystal structure suggests that residues in the 231-to-259 region are necessary because they affect the interaction of λ1 with the threefold and/or fivefold copies of σ2. An effective system for studies of reovirus core structure, assembly, and functions is hereby established.

The orthoreovirus (reovirus) core particle is a molecular machine that mediates synthesis (transcription), 5′-end modification (capping), and export of the 10 viral mRNAs (capped plus strand transcripts), as well as import of the substrates, nucleoside triphosphates and *S*-adenosyl-L-methionine, to produce those mRNAs (53). The core does not include machinery to polyadenylate the mRNAs, which instead terminate with the conserved 3′ pentanucleotide UCAUC (4, 5, 28). The templates for plus strand synthesis are the minus strands of the 10 linear double-stranded RNA (dsRNA) segments that constitute the reovirus genome and that are retained within the core throughout the transcription cycle (1, 51, 55). Further studies of core structure and functions are needed to understand how the different components of this machine are organized to allow for controlled movements of the large template and product RNAs during the multiple rounds of mRNA synthesis that cores can routinely execute from each genome segment (55). Even less is known about how this machine undergoes assembly. The assembly of the three major proteins of reovirus cores to generate core-like particles (CLPs) in a foreign expression system is the subject of this report.

As demonstrated by the reovirus core crystal structure (50), the asymmetric unit from which the icosahedral capsid is built includes an asymmetric dimer of the 142-kDa λ1 protein. Five of these λ1 dimers surround each of the 12 fivefold axes in cores, and these decamers may represent subassemblies from which the full T=1 capsid is later built (60 λ1 dimers in total) (29, 50). Two proteins sit atop the λ1 shell in cores: a pentameric turret of the 144-kDa λ2 protein around each fivefold axis (60 total λ2 subunits per core) and monomeric nodules of the 47-kDa σ2 protein around or across each of the icosahedral symmetry axes, five surrounding and contacting the base of the λ2 turret around each fivefold axis (σ2.5), three around each threefold axis (σ2.3), and one across each twofold axis (σ2.2) (150 total σ2 subunits per core) (50). These σ2 subunits may serve as clamps that hold the λ1 shell together (31), with σ2.5 bridging λ1 subunits from the same decamer and σ2.3 and σ2.2 bridging λ1 subunits from adjacent decamers (50). The two remaining proteins in cores are structurally minor in that they are present in lower copy numbers than the others: 12 copies of the 142-kDa λ3 protein and an estimated 12 to 24 copies of the 83-kDa μ2 protein (14). The precise locations of these last two core proteins remain to be defined, but a variety of evidence including that from X-ray crystallography (50) and transmission cryoelectron microscopy (cryoEM) (18) places both λ3 and μ2 near the fivefold axes, directly beneath and probably

* Corresponding author. Mailing address: Department of Microbiology and Molecular Genetics, Harvard Medical School, 200 Longwood Ave., Boston, MA 02115. Phone: (617) 432-4829. Fax: (617) 738-7664. E-mail: mnibert@hms.harvard.edu.

† Present address: Department of Cellular and Structural Biology, The University of Texas Health Science Center at San Antonio, San Antonio, TX 78229-3900.

‡ Present address: Nature Medicine, New York, NY 10010-1707.

anchored to the λ1 shell. The 10 dsRNA genome segments are coiled within the core interior in a fairly dense, yet poorly understood, arrangement (18, 19, 50).

Not discussed above is information from the core crystal structure about the amino (N)-terminal 200 to 300 amino acids of λ1. The two λ1 subunits within each asymmetric unit are arranged such that one subunit approaches the fivefold axis (λ1.5), whereas the other subunit is excluded from the fivefold area and instead approaches the threefold axis (λ1.3) (50). As a result, five λ1.5 subunits from the same decamer surround each fivefold axis and one λ1.3 subunit from each of three different decamers surrounds each threefold axis. In the core crystal structure, the N-terminal 240 amino acids of the λ1.5 subunits are not seen and thus must be irregularly placed relative to the core's overall icosahedral symmetry (50). In contrast, all but a few of these N-terminal amino acids of the λ1.3 subunits are seen in the crystal structure and take the form of long threadlike arms that extend from their subunits of origin and progressively underlie, and make major contacts with, each of the two other λ1.3 subunits around each threefold axis (50) (see Fig. 10). These arms, by linking the subunits from the three different decamers around each threefold axis, may play an important role in assembling the T=1 λ1 shell. Their extended conformation is consistent with a sequence-based observation that the N-terminal 150 to 200 residues of λ1 are much more hydrophilic on average than the rest of the protein (27).

It has been proposed that four of the five core proteins (λ1, λ2, λ3, and μ2) act as enzymes during viral mRNA synthesis. λ3 is the RNA-dependent RNA polymerase that synthesizes the plus strand transcripts (17, 46, 57; Y. Tao, D. L. Farsetta, M. L. Nibert, and S. C. Harrison, submitted for publication), whereas λ2 is the capping enzyme that mediates the RNA guanylyltransferase, 7-*N*-methyltransferase, and 2′-*O*-methyltransferase activities that complete formation of the 5′ cap as each transcript is exported from the core (13, 22, 32, 39, 41, 50, 52). The roles of λ1 and μ2 are less clear. It has been reported that the N-terminal 440 residues of λ1 include six motifs shared with helicase superfamily I proteins, including the nucleoside triphosphate-binding A and B motifs (7, 48). Both genetic and biochemical studies have suggested that λ1 has nucleoside triphosphatase (NTPase), RNA 5′-triphosphatase, and/or RNA helicase activities, presumably associated with the N-terminal region of λ1 (7, 8, 48). From the core crystal structure, however, we know that this N-terminal region is not seen in the λ1.5 subunits and assumes an extended conformation that makes it unlikely to play an enzymatic role in the λ1.3 subunits (50). Genetic studies have suggested a role for μ2 as well in modulating the NTPase and transcriptase activities of cores (49, 63). Thus, the functional relationship between λ1 and μ2 and their relative roles in aiding the λ3 polymerase in transcription and in mediating the first reaction in mRNA capping (RNA 5′-triphosphatase) remain in some question.

For several other viruses, including other *Reoviridae* family members from the *Rotavirus* and *Orbivirus* genera (15, 20, 33, 38, 47), coexpression of the viral capsid proteins from recombinant baculoviruses allows the assembly of CLPs or virion-like particles (VLPs), depending on which proteins were expressed. These particles have been purified and used to address important questions about their structure, assembly, and enzymatic activities (23, 30, 34, 37, 58, 64–66). The genomic dsRNA segments have not yet been incorporated into particles by following this approach. In reovirus-infected cells, the production of top component (TC) virions, which lack the dsRNA genome, suggests that assembly of the reovirus capsids can also occur independently of genome assembly (18, 21, 56). Indeed, mammalian reovirus CLPs were shown to assemble in HeLa cells when the three major core proteins λ1, λ2, and σ2 were coexpressed by using recombinant vaccinia viruses (61). These reovirus CLPs, which seem likely to be useful for addressing several types of questions about the core, have however been subjected to only limited characterizations to date (61).

In this report, we used recombinant baculoviruses to express reovirus core proteins λ1, λ2, and σ2 in insect cells. The CLPs that resulted were purified and characterized and found to be similar to cores with regard to their sizes, morphologies, and protein compositions. Like cores, the CLPs could also be coated with the two major outer-capsid proteins, μ1 and σ3, to produce VLPs. To begin to use this system to expand our understanding of particle functions and assembly, we addressed the hypothesis that the hydrophilic N-terminal arms of the λ1.3 subunits play an important role in assembling the core shell. We showed that a large N-terminal portion of λ1 is in fact dispensable for CLP assembly but that residues in the 231-to-259 region are required, possibly because they are necessary for the interaction between the λ1.3 and σ2.3 and/or λ1.5 and σ2.5 subunits. An effective system for studies of reovirus core structure, assembly, and functions is hereby established.

MATERIALS AND METHODS

Cells. Spinner-adapted murine L929 cells were grown in suspension in Joklik's modified minimal essential medium (Irvine Scientific, Irvine, Calif.) supplemented to contain 2% fetal bovine serum (HyClone Laboratories, Logan, Utah), 2% neonatal bovine serum (HyClone), 2 mM glutamine (Irvine Scientific), and 100 U of penicillin per ml and 100 μg of streptomycin per ml (Irvine Scientific). *Spodoptera frugiperda* 21 and *Trichoplusia ni* High Five insect cells (Invitrogen, Carlsbad, Calif.) were grown in TC-100 medium (Gibco BRL, Gaithersburg, Md.) supplemented to contain 10% heat-inactivated fetal bovine serum.

Virions, TC virions, and cores. Purified virions, TC virions, and cores of reovirus strain type 1 Lang (T1L) were obtained, stored, and quantitated as previously described (21). The protein compositions of the particles were confirmed by sodium dodecyl sulfate-polyacrylamide gel electrophoresis (SDS-PAGE) (see below).

Dual recombinant baculovirus containing the reovirus T1L L3 and S2 genes. The cloning of the T1L L3 gene into the pBlueScript II KS vector (Stratagene, La Jolla, Calif.) to yield pBS-$L3_L$ was previously reported (27). For cloning the T1L S2 gene, viral transcripts produced by T1L cores were first copied by avian myeloblastosis virus reverse transcriptase (Gibco BRL). For this reaction, the primer was complementary to the 3′ end of S2 plus strand and included an *Xho*I site, not otherwise present in the T1L S2 gene, near its 5′ end (5′-CCGCTCGAGGATGAATGTGTGGTCAGTCG-3′; *Xho*I site underlined). The resulting single-stranded cDNA was subjected to second-strand synthesis by the Klenow fragment of *Escherichia coli* DNA polymerase I (New England Biolabs, Beverly, Mass.). For this reaction, the primer was complementary to the 3′ end of S2 gene minus strand and again included an *Xho*I site near its 5′ end (5′-CCGCTCGAGGCTATTCGCTGGTCAGTTAT-3′ for S2; *Xho*I site underlined). The resulting double-stranded cDNA was digested with *Xho*I, end filled with Klenow fragments, and subcloned into the *Sma*I site of pBluescript II KS to generate pBS-$S2_L$ (due to unexplained difficulty in cloning into the *Xho*I site). The sequence of the S2 DNA clone used in these studies was shown to be identical to that previously reported for the T1L S2 genome segment (16).

To generate a dual-recombinant baculovirus to coexpress λ1 and σ2, the T1L L3 gene was excised from pBS-$L3_L$ by *Eco*RI and subcloned into the *Eco*RI site of the pFastbacDual vector (pFbD) (Gibco BRL). In the resulting pFbD-$L3_L$ plasmid, the L3 gene was positioned under the transcription control of the

baculovirus (*Autographica californica* nuclear polyhedrosis virus [AcMNPV]) polyhedrin promoter. The T1L S2 gene was excised by *Eco*RV and *Not*I from pBS-$S2_L$ and subcloned into the same sites of the pcDNAI vector (Invitrogen). The resulting pcDNAI-$S2_L$ plasmid was digested with *Eco*RV and *Sph*I, and the S2 gene-containing fragment was subcloned into the *Sma*I and *Sph*I sites of pFbD-$L3_L$. In the resulting pFbD-$L3_LS2_L$ plasmid, the S2 gene was positioned under the transcription control of the baculovirus (AcMNPV) p10 promoter. To generate pFbD-$S2_L$, the L3 gene was removed from pFbD-$L3_LS2_L$ by excision with *Eco*RI. The pFbD-$L3_L$, pFbD-$L3_LS2_L$, and pFbD-$S2_L$ plasmids were used to generate the corresponding three recombinant baculoviruses (Bac-$\lambda1_L$, -$\lambda1_L\sigma2_L$, and -$\sigma2_L$) with the Bac-to-Bac system (Gibco BRL). The baculoviruses were amplified into high-titer stocks by serial passage in *S. frugiperda* 21 cells.

Expression of λ1, σ2, and λ2 in *S. frugiperda* 21 cells. *S. frugiperda* 21 cells (7.5×10^6) on a 100-cm^2 dish were infected with third-passage lysate stocks of each recombinant baculovirus at a multiplicity of infection (MOI) of 5 to 10. Bac-$\lambda1_L$, Bac-$\sigma2_L$, Bac-$\lambda2_D$ (39, 41), Bac-$\lambda1_L\sigma2_L$, or Bac-$\lambda1_L\sigma2_L$ and Bac-$\lambda2_D$ were used to express λ1; σ2; λ2; λ1 and σ2; or λ1, σ2, and λ2, respectively. At 72 h postinfection (p.i.) the cells were pelleted at 500 × *g* for 10 min at 40°C and washed twice with cold phosphate-buffered saline (PBS) (137 mM NaCl, 3 mM KCl, 8 mM Na_2HPO_4, 1 mM KH_2PO_4 [pH 7.5]). The pellet was resuspended in 800 μl of cold lysis buffer (100 mM NaCl, 5 mM $MgCl_2$, 20 mM Tris-HCl, 1% Triton X-100, 5 μg of leupeptin/ml, 1 mM phenylmethylsulfonyl fluoride [pH 7.4]) and incubated on ice for 30 min. The soluble, cytoplasmic fraction was separated from the insoluble cellular debris and nuclear fraction by centrifugation at 500 × *g* for 10 min at 40°C. The expression level of each protein as determined by SDS-PAGE and immunoblotting reached a maximum at approximately 48 h p.i. and remained approximately constant until at least 84 h p.i.

Polyclonal antiserum against λ1. The T3D L3 gene was excised from pBS-$L3_D$ (27) at its *Bam*HI and *Hin*dIII sites and subcloned into the same sites in the pET-21b expression plasmid (Novagen, Madison, Wis.) to generate plasmid pET-21b-$L3_D$. pET-21b-$L3_D$ was transformed into BL21-DE3 cells (Novagen), followed by the expression protocol described in the pET system manual (Novagen). The expression of the λ1 protein directed from pET-21b-$L3_D$ was induced at the mid-log cell phase by adding isopropyl-β-D-thiogalactopyranoside to 0.5 mM. After incubation at 37°C for 3 h, cells were harvested by centrifugation at 7,800 × *g* for 5 min, resuspended in cold PBS containing 1× protease inhibitor cocktail (Roche Applied Science, Indianapolis, Ind.), and lysed by sonication. The inclusion bodies containing λ1 were crudely purified from the lysate by centrifugation at 8,000 × *g* for 30 min through a 20% sucrose cushion. SDS-PAGE and immunoblotting with a rabbit antiserum raised against heat-inactivated reovirus cores (11; S. Noble and M. L. Nibert, unpublished data) demonstrated that λ1 constituted around 70% of these inclusion bodies. To purify λ1 further, an electroelution protocol was applied (25). The eluant was concentrated by solvent absorption with polyethylene glycol. The polyclonal antiserum was produced in a rabbit injected with the electroeluted and concentrated λ1 protein at the Animal Care Unit of the University of Wisconsin Medical School (Madison).

SDS-PAGE and immunoblot analysis. All samples were mixed 1:2 with 3× sample buffer (375 mM Tris, 3% SDS, 6% β-mercaptoethanol, 30% sucrose, 0.03% bromophenol blue [pH 8.0]), disrupted by boiling for 3 min, and separated in an SDS–10% polyacrylamide gel by electrophoresis. Staining was performed with Coomassie brilliant blue R-250 (Sigma Chemical, St. Louis, Mo.). For immunoblotting, proteins in the gel were electrophoretically transferred onto a nitrocellulose membrane (Bio-Rad Laboratories, Hercules, Calif.) in the presence of transfer buffer (25 mM Tris, 192 mM glycine, pH 8.3) at 4°C for 1 h at 100 V. As a source of primary antibodies, the rabbit polyclonal anti-λ1 serum was used at 1:10,000 to detect λ1, the rabbit polyclonal anti-core serum was used at 1:500 to detect σ2, and the mouse monoclonal antibody 7F4 (60) was used at 1 μg/ml to detect λ2. Secondary antibodies were alkaline phosphatase-coupled goat anti-rabbit immunoglobulin or goat anti-mouse immunoglobulin (Bio-Rad), and *p*-nitroblue tetrazolium chloride and 5-bromo-4-chloro-3-indolylphosphate *p*-toluidine (Bio-Rad) in reaction buffer (100 mM Tris, 0.5 mM $MgCl_2$ [pH 9.5]) were used for detection.

Generation and purification of CLPs from *S. frugiperda* 21 cell lysates. To generate λ1σ2λ2 CLPs, 2.4×10^8 *S. frugiperda* 21 cells were coinfected with Bac-$\lambda1_L\sigma2_L$ and Bac-$\lambda2_D$, each at an MOI of 5 to 10. Because the λ1, σ2, and λ2 proteins from reoviruses T1L and T3D can viably associate in reassortant viruses (17, 48, 49, 63), the mixture of T1L λ1 and σ2 with T3D λ2 in these experiments was not expected to interfere with particle assembly and did not do so. Cells were harvested at 72 h p.i., washed twice with cold PBS, and resuspended in cold A buffer (1 M NaCl, 50 mM Tris-HCl [pH 8.0]) containing a 1× protease inhibitor cocktail. Either directly or after freezing and thawing, cells were lysed by sonication and incubated on ice for 30 min after sodium deoxycholate was added to 0.1%. Freon extraction was then performed three or four times, and the CLPs were purified from the supernatant through a 1.25- to 1.35-g/cm^3 CsCl equilibrium gradient. Centrifugation was performed for 3 h or more at 5°C with a Beckman SW41 or SW28.1 rotor at a speed of 35,000 or 25,000 rpm, respectively. The distinct particle bands were harvested and dialyzed against virion buffer for storage. To purify CLPs consisting of λ1 and σ2 (λ1σ2 CLPs), similar numbers of *S. frugiperda* 21 cells were infected with Bac-$\lambda1_L\sigma2_L$ alone and subsequently processed as described above. Unsuccessful attempts to make and purify λ1-only CLPs were performed in the same manner with Bac-$\lambda1_L$.

Negative-stain transmission electron microscopy (EM). Copper 400-mesh Formvar carbon-coated grids were used for particle adsorption. A grid was floated on a drop (~50 μl) of sample solutions for 5 min and then washed twice with PBS. In each step, excess fluid was absorbed with filter paper. The grids were stained in a drop of freshly filtered 1% uranyl acetate and observed with a Philips 120 transmission electron microscope at 100 kV as described previously (10).

Transmission cryoEM and image reconstruction. Purified CLPs were embedded in vitreous ice, and micrographs were taken below −176°C at a dose of ~21 electrons/$Å^2$ in a Philips CM200 field emission gun microscope at a magnification of ×38,000 and defocus values ranging between 2.5 and 3.4 μm underfocus. The T1L core images from a previous study (19) were reprocessed as described below. The particle orientations and centers were determined by using a model-based method (2). Three-dimensional (3D) reconstructions were computed to 32-Å resolution as described previously (3) from 54 and 769 particle images for the core and CLP samples, respectively. The particle orientations in both reconstructions were randomly distributed in the asymmetric unit as evidenced by the eigenvalue spectra where all inverse eigenvalues were <0.10 and more than 99% were <0.01 (3). As the CLP data included images recorded at different defocus levels, the reconstruction of the CLP was computed with adjustments made to compensate in part for the effects of the microscope contrast transfer function (3).

Construction of λ1 (L3) deletion mutants. For easy manipulation, the T1L L3 gene and surrounding sequences were excised from pFbD-$L3_LS2_L$ at the *Sma*I and *Spe*I sites and subcloned into the *Sma*I and *Xba*I sites of pGEM-4Z (Promega, Madison, Wis.) to generate pGEM-4Z-$L3_L$. This plasmid was used as template for all inverse PCRs applied to generate a series of deletion mutants. With some modifications from the published protocol (62), inverse PCR was performed with the following conditions: step 1, 95°C, 30 s; step 2, 95°C, 30 s; step 3, 54°C, 1 min; step 4, 68°C, 15 min; there were 20 cycles of steps 2 to 4. The 50 μl of reaction mixture contained 0.1 μg of pGEM-4Z-$L3_L$, 10 pmol of each forward and reverse primer, 0.2 mM deoxynucleoside triphosphate, 2.5 U of *Pfu* polymerase (Stratagene), and 1× *Pfu* buffer supplied by the manufacturer. Each PCR product was end filled with 5 U of Klenow fragment (New England Biolabs) in an effort to increase the population of full-length, blunt-end product and then treated with *Dpn*I for 2 h at 37°C. After this, the product was cut with *Nco*I if required (see below), isolated on a 0.8% agarose gel, purified from the gel slice, and self-ligated to reconstitute the circular plasmid.

For each inverse PCR to generate a T1L L3 gene encoding λ1Δ2-26, λ1Δ2-176, λ1Δ2-200, or λ1Δ2-230, the reverse primer (5′-CCATGGCATCCTGACG ATTAGCG-3′; complementary to the 5′-nontranslated region of the T1L L3 gene with an additional *Nco*I site as underlined) was paired with the following forward primers: 5′-CCATGGTCGAGCCAATTACGAGAC-3′ for λ1Δ2-26, 5′-CCATGGAGTGGTCATGGGTATCAG-3′ for λ1Δ2-176, 5′-CCATGGGC CTCACATGGTTTGCATGG-3′ for λ1Δ2-200, and 5′-CCATGGCCTATTGT TCAAGTTTCGGC-3′ for λ1Δ2-300 (*Nco*I site in each is underlined). After *Dpn*I treatment, the products were cut with *Nco*I before gel isolation and self-ligation. Sequencing confirmed that the resulting clones pGEM-4Z-$L3_L$Δ2-26, -Δ2-176, -Δ2-200, and -Δ2-230 had the correct sequences from the *Nco*I site to either the *Nhe*I (for pGEM-4Z-$L3_L$Δ2-26) or the *Bpu*1102I (for pGEM-4Z-$L3_L$Δ2-176, -Δ2-200, and -Δ2-230) site. As expected from the sequences of the PCR primers, six additional nucleotides (two amino acids, Pro and Trp) originating from the *Nco*I site were inserted after the λ1 start codon in these clones. The *Rsr*II-*Nhe*I or *Rsr*II-*Bpu*1102I fragment of pFbD-$L3_LS2_L$ was replaced with the *Rsr*II-*Nhe*I fragment from pGEM-4Z′-$L3_L$Δ2-26 or the *Rsr*II-*Bpu*1102I fragments from pGEM-4Z-$L3_L$Δ2-176, -Δ2-200, or -Δ2-230 to generate pFbD-($L3_L$Δ2-26)$S2_L$, -($L3_L$Δ2-176)$S2_L$, -($L3_L$Δ2-200)$S2_L$, and -($L3_L$Δ2-230)$S2_L$, respectively. These pFbD plasmids were then used to generate the corresponding dual-recombinant baculoviruses [Bac-($\lambda1_L$Δ2-26)$\sigma2_L$, -($\lambda1_L$Δ2-176)$\sigma2_L$, -($\lambda1_L$Δ2-200)$\sigma2_L$, and -($\lambda1_L$Δ2-230)$\sigma2_L$] as described above for Bac-$\lambda1_L\sigma2_L$.

For inverse PCR to generate the λ1Δ2-260 deletion, the reverse primer (5′-CATCCTGACGATTAGC-3′) was paired with the forward primer (5′-GCTGG TTTGTGTACTTCG-3′). After *Dpn*I treatment, the products were subjected to gel isolation and self-ligation. The resulting clone, pGEM-4Z-$L3_L$Δ2-260, was

sequenced to confirm that there were no other mutations between the λ1 start codon and the *Bpu*1102I site. The *Rsr*II-*Bpu*1102I fragment from this plasmid was then substituted for the same fragment of pFbD-$L3_LS2_L$ to generate pFbD-$L3_L\Delta2\text{-}260S2_L$.

To introduce the λ1Δ2-315 deletion into the T1L L3 gene, a regular PCR was carried out by using pBS-$L3_L$ as the template, forward primer 5′-CGGTCCGG CTAATCGTCAGGATGGACTTTGACCGAGATTCG-3′ (*Rsr*II site single underlined, codons of methionine 1 and aspartate 314 double underlined), and reverse primer 5′-CGTGGCCACGTGTGAGGCG-3′ (*Msc*I site underlined). The PCR product was cut with *Rsr*II and *Msc*I and then substituted for the *Rsr*II-*Msc*I fragment of pBS-$L3_L$, generating pBS-$L3_L\Delta2\text{-}315$. Sequencing confirmed that the amplified fragment contained the expected deletion and that no other mutations had been introduced. The *Rsr*II-*Msc*I fragment from this plasmid was then excised and subcloned into pFbD-$L3_LS2_L$ to generate pFbD-$(L3_L\Delta2\text{-}315)S2_L$, which was then used to generate recombinant baculovirus Bac-$(\lambda1_L\Delta2\text{-}315)\sigma2_L$.

Purification of VLPs from the cell lysates. To obtain a cell lysate containing the two outer-capsid proteins μ1 and σ3, 8×10^7 *T. ni* High Five cells were infected with Bac-$\mu1_L\sigma3_L$ (11) at an MOI of 5 to 10. Cells harvested at 60 h p.i. were washed twice with cold PBS and resuspended in cold B buffer (100 mM NaCl, 50 mM Tris, pH 8.0) containing 1× protease inhibitor cocktail. After being frozen and thawed, the cells were lysed and homogenized by sonication. This cell lysate containing μ1 and σ3 was then mixed with a cell lysate containing λ1σ2λ2 CLPs, generated as described in a preceding section. The mixture was incubated at 37°C for 1 h with stirring every 15 min and then placed on ice to cool and incubated for 30 min further on ice after adding sodium deoxycholate to 0.1%. The mixture was next extracted with Freon and subjected to a CsCl gradient as described for CLPs in a preceding section. The resulting particle bands on the gradient were harvested and dialyzed against virion buffer for storage. Unsuccessful attempts to coat λ1σ2 CLPs were performed in the same manner and also by using a modification in which A buffer (see above) was substituted for B buffer.

RESULTS

Expression of the three major reovirus core proteins using recombinant baculoviruses. A previous study using recombinant vaccinia viruses for protein expression (61) indicated that both the core shell protein λ1 and the core nodule protein σ2 are required to assemble reovirus CLPs. For the present study λ1 and σ2 were therefore commonly coexpressed by using the dual-recombinant baculovirus Bac-$\lambda1_L\sigma2_L$ rather than by using the two single-recombinant baculoviruses Bac-$\lambda1_L$ and Bac-$\sigma2_L$. The core turret protein λ2 was expressed by using the single-recombinant baculovirus Bac-$\lambda2_D$ as described previously (39, 41). Although SDS-PAGE of lysates from the baculovirus-infected insect cells failed to show the recombinant λ1, σ2, and λ2 bands clearly, due to their low expression levels (Fig. 1a), immunoblotting using the appropriate polyclonal antiserum or monoclonal antibody demonstrated each of these proteins in the lysates (Fig. 1b). λ1 was detected only in cells infected with Bac-$\lambda1_L$ or Bac-$\lambda1_L\sigma2_L$ (Fig. 1b, lanes 3, 6, and 7), λ2 was detected only in cells infected with Bac-$\lambda2_D$ (Fig. 1b, lanes 5 and 7), and σ2 was detected only in cells infected with Bac-$\sigma2_L$ or Bac-$\lambda1_L\sigma2_L$ (Fig. 1b, lanes 4, 6, and 7).

Isolation of λ1σ2 and λ1σ2λ2, but not λ1-only, CLPs. In an effort to purify the CLPs expected to be formed in baculovirus-infected insect cells expressing the reovirus core proteins, the method for purifying infectious virions from reovirus-infected L cells (21) was modified (see Materials and Methods). In the CsCl gradient that made up the final step of the protocol, four or five closely migrating bands, each similar in appearance to the bands representing purified virions or TC virions from infected L cells (18, 21), were routinely obtained from the insect cell lysates in which either λ1 and σ2 or λ1, σ2, and λ2 had been expressed (Fig. 2a and data not shown). The buoyant

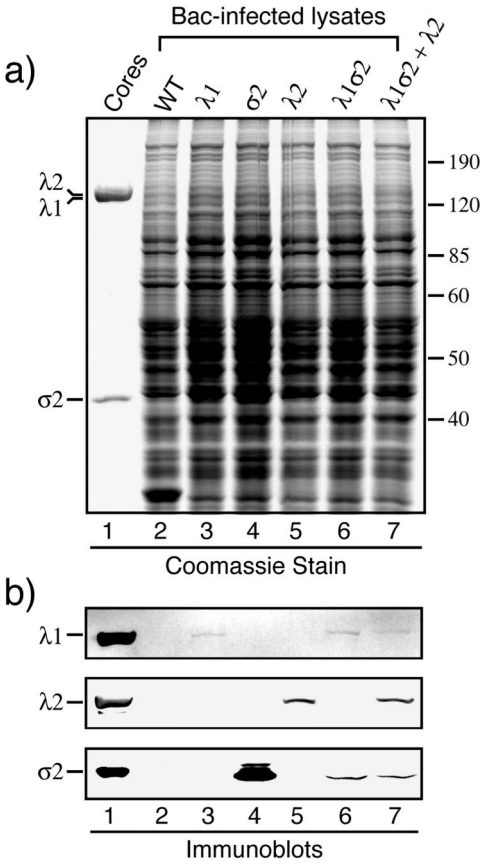

FIG. 1. Expression of the three reovirus core proteins in insect cells using recombinant baculoviruses. *S. frugiperda* 21 cells were infected with wild-type (WT) baculovirus (lane 2), Bac-$\lambda1_L$ (lane 3), Bac-$\sigma2_L$ (lane 4), Bac-$\lambda2_D$ (lane 5), Bac-$\lambda1_L\sigma2_L$ (lane 6), or Bac-$\lambda1_L\sigma2_L$ and Bac-$\lambda2_D$ (lane 7). The cells were harvested at 72 h p.i. and lysed. (a) The soluble cytoplasmic fractions were analyzed by SDS-PAGE and Coomassie staining. Reovirus T1L core particles (lane 1) were included on the gel to mark the positions of the core proteins. All three λ proteins (142 to 144 kDa each) comigrate in one band in this type of gel. (b) The same samples, including core particles, were analyzed in the same respective lanes of another gel by SDS-PAGE and immunoblotting using a polyclonal anti-λ1 serum, anti-λ2 monoclonal antibody 7F4, or a polyclonal anti-core serum to detect σ2. Only those portions of the blot containing the respective proteins are shown.

densities of these bands were measured by refractometer to be in the range of 1.29 to 1.31 g/cm^3 (data not shown), and the uppermost band was always the predominant one (Fig. 2a and data not shown). For the characterizations in this study, all of these bands were harvested together.

The protein compositions of the putative CLP bands obtained from insect cells expressing either λ1 and σ2 or λ1, σ2, and λ2 were analyzed and compared with that of authentic core particles by SDS-PAGE and immunoblotting. In Coomassie brilliant blue-stained gels, the putative λ1σ2 CLPs (Fig. 3a, lane 2) and λ1σ2λ2 CLPs (Fig. 3a, lane 3) each showed two major protein bands, which comigrated with the λ band (containing the λ1, λ2, and λ3 proteins) and σ2 band of core particles (Fig. 3a, lane 1). Immunoblots of the same gel confirmed that the slow-migrating band contained λ1 in the putative λ1σ2 CLPs and both λ1 and λ2 in the putative λ1σ2λ2

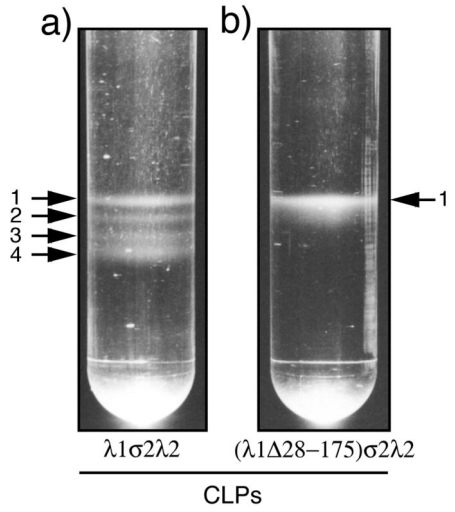

FIG. 2. Appearance of putative CLP bands in CsCl gradients. *S. frugiperda* 21 cells were infected with Bac-$\lambda 1_L\sigma 2_L$ and Bac-$\lambda 2_D$ (a) or Bac-$\lambda 1_L(\Delta 28\text{-}175)\sigma 2_L$ and Bac-$\lambda 2_D$ (b). The cells were harvested at 72 h p.i. and processed. The CLPs putatively contained within the cell lysates were allowed to form discrete bands, visible by eye, on a 1.25- to 1.35-g/cm^3 CsCl equilibrium gradient and then photographed. Arrows, numbers of discrete bands visible in each gradient. The upper parts of the tubes have been cropped from these images but contained no visible bands.

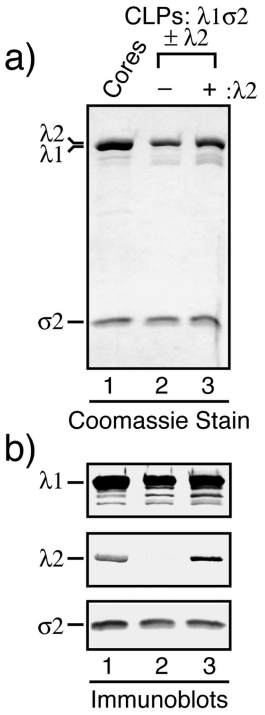

FIG. 3. Protein compositions of purified CLPs. CLPs were purified from the lysate of *S. frugiperda* 21 cells infected with either Bac-$\lambda 1_L\sigma 2_L$ (lane 2) or Bac-$\lambda 1_L\sigma 2_L$ and Bac-$\lambda 2_D$ (lane 3). (a) The CLPs were analyzed by SDS-PAGE and Coomassie staining to estimate their protein contents. Reovirus T1L core particles (lane 1) were included on the gel to mark the positions of the core proteins as well as to provide a standard for the relative intensities of the λ and σ2 bands. (b) The same samples, including core particles, were analyzed in the same respective lanes of another gel by SDS-PAGE and immunoblotting as described for Fig. 1b.

CLPs, whereas the fast-migrating band contained σ2 in each (Fig. 3b). The densitometric ratio of the slow-migrating band to the fast-migrating band in λ1σ2λ2 CLPs was somewhat less than that in cores, at least partly due to the absence of λ3 from the CLPs (data not shown). Small amounts of λ1 degradation products with slightly lower molecular weights than the full-length protein were detected by immunoblotting in both types of CLPs as well as in cores (Fig. 3b). No detectable levels of other proteins were consistently evident. Together with the observation that λ1σ2λ2 CLPs migrated in sucrose gradients at a rate similar to that for TC virions (data not shown), these results are consistent with the successful interaction of the major viral core proteins in insect cells and subsequent purification of both λ1σ2 and λ1σ2λ2 CLPs to a high level of purity.

We made multiple attempts to assemble CLPs with λ1 alone. The reovirus core crystal structure shows that the 60 λ1 dimers form a complete shell, whereas λ2 and σ2 bind atop it (50). It is thus reasonable to hypothesize that expression of λ1 alone might lead to CLP formation. Xu et al. (61) reported, however, that expression of λ1 alone did not yield CLPs in the recombinant vaccinia virus system. Like those authors, we obtained no evidence for CLP formation after expression of λ1 alone in the recombinant baculovirus system: particle bands were not observed in the CsCl gradient used as the final step in the purification procedure (data not shown). This is consistent with the previous conclusion (61) that λ1 and σ2 constitute the minimal reovirus components to assemble CLPs.

Negative-stain EM of CLPs. To determine whether the purified CLPs have morphology similar to that of cores, EM was performed with 1% uranyl acetate as the negative stain. Core particles of reovirus T1L were used as a positive control (Fig. 4a). The purified λ1σ2λ2 CLPs (Fig. 4b) appeared similar to cores in that they had a uniform diameter of 50 to 60 nm and their single protein layers were continuous and thinner than those of TC virions, which have both inner and outer capsids (Fig. 4c) (21, 56). Together with the previous SDS-PAGE and immunoblot results (Fig. 3), these findings suggest the purified λ1σ2λ2 CLPs have a single continuous protein layer consisting of λ1 and σ2, consistent with the X-ray structure of cores (50). However, the negative-stain images in this study failed to provide clear views of the λ2 turrets on either CLPs or cores, which might be explained by the poor resolution of this analysis. It was also noteworthy that the stain penetrated into the interior cavity of the CLPs (Fig. 4b), as into TC virions that lack the dsRNA genome (Fig. 4c), but that cores packed with the dsRNA genome were more impermeable to the stain (Fig. 4a) (18, 21, 56). This indicates that the purified CLPs allow small molecules of stain to enter and be deposited in their interior cavities, which thus appear mostly devoid of other components such as RNA (but see Discussion). CLPs also behaved like cores in that they reversibly aggregated and disaggregated when placed in low- and high-ionic-strength solutions, respectively (data not shown). Negative-stain EM images of λ1σ2 CLPs showed that they have a morphology similar to that of λ1σ2λ2 CLPs and cores but a stronger tendency to aggregate, as previously noted for spikeless cores from which

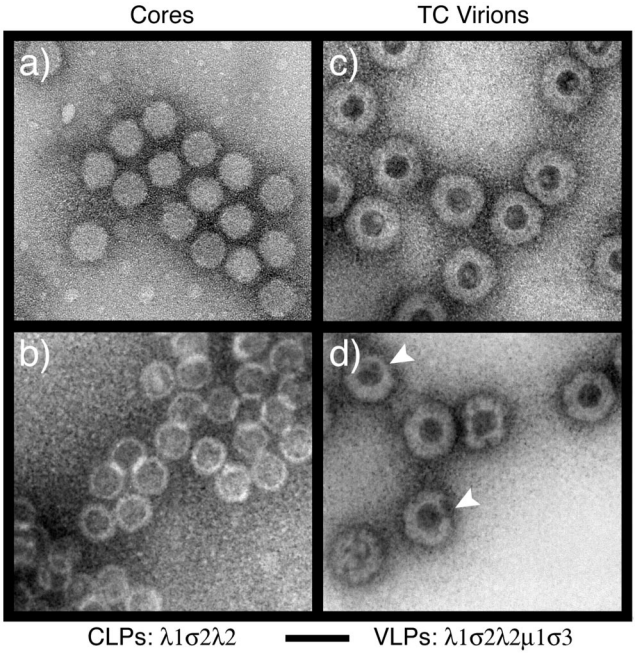

FIG. 4. Transmission electron micrographs of negatively stained reovirus particles. Purified T1L cores (a), λ1σ2λ2 CLPs (b), T1L TC virions (c), and λ1σ2λ2μ1σ3 VLPs (d) were absorbed onto carbon-coated copper grids, stained with 1% uranyl acetate, and observed by EM. Arrowheads (d), partially coated VLPs. Bar, 100 nm.

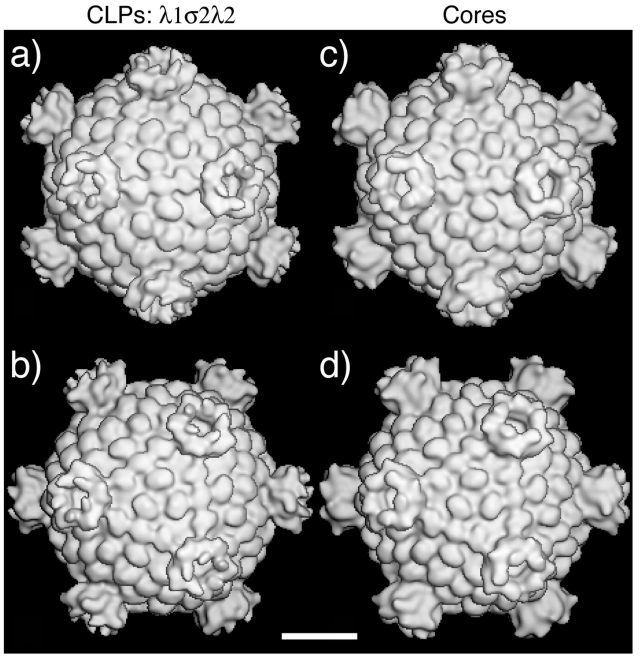

FIG. 5. 3D reconstructions of reovirus particles obtained by image processing of transmission cryoelectron micrographs. Purified λ1σ2λ2 CLPs (a and b) and T1L cores (c and d) were examined. Each reconstruction is shown as a surface-shaded view down either a twofold axis (a and c) or a threefold axis (b and d) at a resolution of 32 Å. Bar, 20 nm.

the λ2 turrets had been removed biochemically (42) (data not shown).

CryoEM and three-dimensional (3D) image reconstruction of CLPs. Since the λ2 turrets on neither λ1σ2λ2 CLPs nor cores were well visualized by negative-stain EM in this study, we performed cryoEM and image reconstruction to identify more details of the structural similarity between CLPs and cores preserved in a vitrified state and observed in three dimensions. Surface views of the purified λ1σ2λ2 CLPs (Fig. 5a and b) looked almost identical to those of purified T1L cores (Fig. 5c and d), including the large pentameric λ2 turrets that project around the fivefold axes and the monomeric σ2 nodules that externally decorate the λ1 shell around the fivefold and threefold axes as well as across the twofold axes. These findings provide evidence that the λ1, σ2, and λ2 proteins were able to assemble into approximately the same structure—and in approximately the same copy numbers—during CLP formation in recombinant baculovirus-infected insect cells as during virion morphogenesis in reovirus-infected mammalian cells.

A notable feature of the CLP reconstruction is that the outer, "flap" domains of the T3D λ2 protein (50) adopt a conformation resembling that of the region of the T1L λ2 in T1L cores (19) (Fig. 5c and d) and TC cores (18) but distinct from that of the region of the T3D λ2 in T3D cores (40, 42). The basis for this difference remains unknown but may relate to differences in preparation conditions (J. Kim, X. Zhang, S. B. Walker, T. S. Baker, and M. L. Nibert, unpublished data). In any case, this finding indicates that the flap domains of T3D λ2 are capable of opening the top of the λ2 "reaction vessel" to a larger extent than previously seen, which may be important for release of capped transcripts (19; M. Yeager, S. Weiner, and K. M. Coombs, abstract from the 40th Annual Meeting of the Biophysical Society, Biophys. J. **70:**A116, 1996).

CLPs formed with N-terminal deletions of λ1. To address the hypothesis that the hydrophilic N-terminal arms of the λ1.3 subunits are important for assembly of the λ1 shell (see the introduction), we designed a series of deletion mutations within the first 315 amino acids of λ1 (Fig. 6). These residues include the first four helicase-like motifs (7, 48) as well as the zinc finger (6, 27, 50). The λ1 mutants from which the five smallest numbers of residues were removed (λ1Δ2-26, λ1Δ28-175, λ1Δ2-176, λ1Δ2-200, and λ1Δ2-230) were all expressed well in insect cells, to levels at least as high as that for full-length λ1 (data not shown). CLPs from insect cell lysates in which each of these λ1 mutants had been coexpressed with σ2 and λ2 were purified in parallel by the procedure for CLP purification described above. In each case, a single particle band was observed (Fig. 2b and data not shown); this band comigrated with the uppermost, predominant band of the CLPs formed with full-length λ1 (buoyant density near 1.29 g/cm^3) (Fig. 2a). Thus, the minor bands observed in the CsCl gradient for CLPs formed with full-length λ1 are attributable to sequences in the N-terminal region of λ1 (see Discussion). SDS-PAGE revealed that the CLPs containing λ1Δ2-26, λ1Δ28-175, λ1Δ2-176, λ1Δ2-200, or λ1Δ2-230 were purified with virtually no detectable cellular protein contamination (Fig. 7a and data not shown). The λ1 deletion mutants migrated at the expected gel position in comparison with the full-length λ1 protein of cores: the λ1Δ2-26 mutant migrated similarly to full-length λ1 because of its small deletion (~3 kDa), whereas the other four mutants migrated faster than

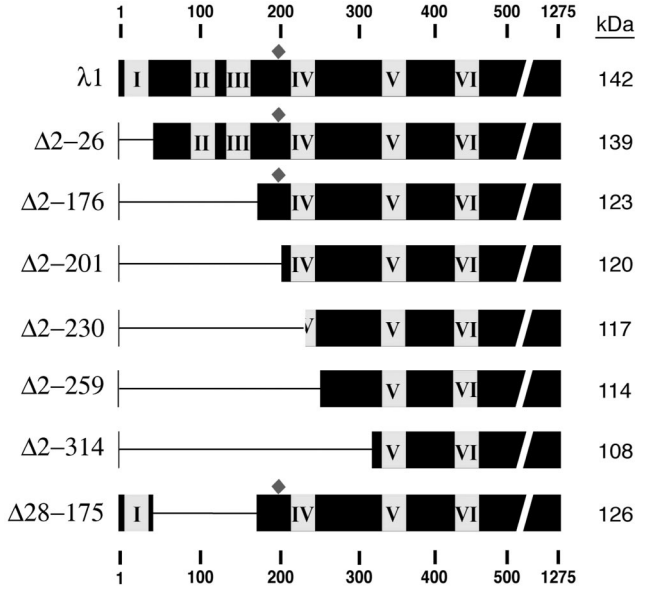

FIG. 6. Schematic diagram of λ1 deletion mutants. Deletions in the T1L L3 gene were constructed in order to express versions of the full-length T1L λ1 protein (1,275 amino acids, 142 kDa) with deletions. The missing region in each deletion mutant is indicated by the horizontal narrow line. As a result of these deletions, the different versions of λ1 differ in expected molecular mass as indicated at the right. Numbers at the top and bottom are residue numbers. Boxes I to VI, positions of the six putative helicase-like motifs (7, 48); diamonds, positions of the zinc finger motifs (6, 27, 50).

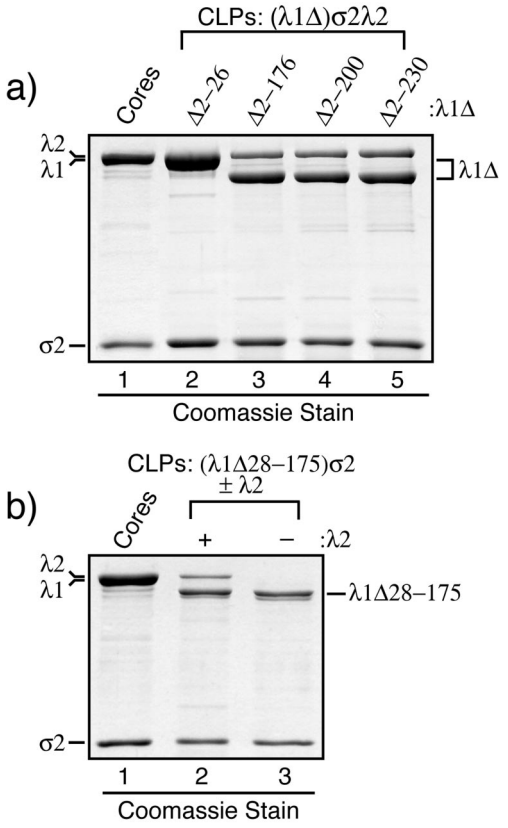

FIG. 7. Protein compositions of purified CLPs formed with the λ1 deletion mutants. CLPs were formed following coexpression of the reovirus core proteins in *S. frugiperda* 21 cells by infections with Bac-$\lambda1_L\Delta2\text{-}26\sigma2_L$, Bac-$\lambda1_L\Delta2\text{-}176\sigma2_L$, Bac-$\lambda1_L\Delta2\text{-}200\sigma2_L$, Bac-$\lambda1_L\Delta2\text{-}230\sigma2_L$, Bac-$\lambda1_L\Delta28\text{-}175\sigma2_L$, and/or Bac-$\lambda2_D$ as indicated. The CLPs were then purified from the infected-cell lysates. (a) Each of the indicated λ1 deletion mutants was coexpressed along with σ2 and λ2. The resulting CLPs were analyzed by SDS-PAGE and Coomassie staining. (b) λ1Δ28-175, as a representative of CLP-positive λ1 deletion mutants, was coexpressed with σ2 in either the presence (+) or the absence (−) of λ2. The resulting CLPs were analyzed by SDS-PAGE and Coomassie staining.

full-length λ1, consistent with their larger deletions of approximately 16, 19, 22, and 25 kDa for λ1Δ28-175, λ1Δ2-176, λ1Δ2-200, and λ1Δ2-230, respectively. As a representative of this group of CLP-positive mutants, λ1Δ28-175 was also used to demonstrate that it can form CLPs with σ2 in the absence of λ2 (Fig. 7b), thereby excluding the possibility that λ2 is needed to assemble or stabilize the CLPs that are formed with these mutants. In sum, these results demonstrate that the N-terminal 230 amino acids of λ1 are dispensable for assembly of the λ1-σ2 shell, which is contrary to the original hypothesis suggested by the core crystal structure (50). These results also demonstrate that the N-terminal 230 amino acids of λ1 are dispensable for incorporation of λ2 on top of the λ1-σ2 shell, which is consistent with the locations of these N-terminal sequences beneath the main λ1 shell in both the λ1.3 and the λ1.5 subunits (50). Since the λ1 zinc finger (residues 181 to 208) was deleted from the λ1Δ2-200 and λ1Δ2-230 mutants, the results further suggest that the unknown function of this zinc finger pertains to something other than core shell assembly.

The λ1 deletion mutants from which the two largest numbers of residues were removed, λ1Δ2-259 and λ1Δ2-314, were also expressed well in insect cells, to nearly the same levels as full-length λ1. However, in three trials with each, we failed to obtain particle bands in the CsCl gradient during the procedure to purify CLPs. These failures suggest that amino acids 231 to 259 are necessary for CLP formation. One possibility is that amino acids in this region are important for maintaining the overall conformation of λ1 so that the deletions spanning this region caused λ1 to be misfolded and thereby not competent for CLP assembly. Another possibility is that amino acids in the 231-to-259 region are important for mediating or affecting specific λ1-λ1 or λ1-σ2 interactions that are essential for CLP assembly.

Complementation of λ1Δ2-259 and λ1Δ2-314 for CLP formation. To address whether the CLP-negative mutants λ1Δ2-259 and λ1Δ2-314 have normal conformations in the parts of λ1 that they contain, we adopted a complementation approach. We hypothesized that if the conformations of λ1Δ2-259 and λ1Δ2-314 are approximately normal, then each may be complemented by full-length λ1 or a CLP-positive λ1 deletion mutant, so that they can be assembled into CLPs that contain both these forms of λ1. In contrast, if λ1Δ2-259 and λ1Δ2-314 are misfolded, then they would not be expected to be assembled into CLPs by complementation. In initial experiments, λ1Δ2-314 was coexpressed with λ1Δ28-175 (a CLP-positive mutant; Fig. 6b), σ2, and λ2. As a control, λ1Δ28-175, σ2, and λ2 were coexpressed in parallel. The resulting CLPs from the two samples were purified in parallel by the usual procedure,

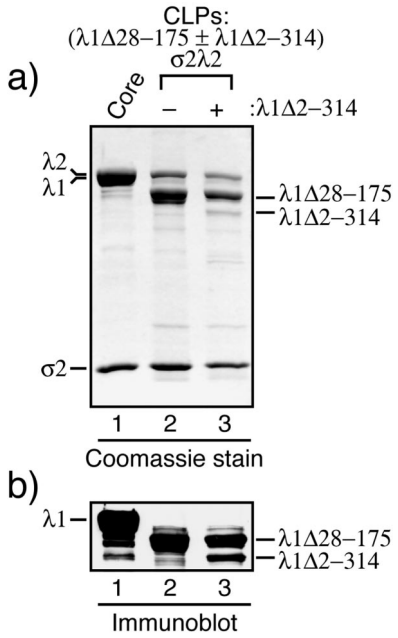

FIG. 8. Complementation of a CLP-negative λ1 mutant with a CLP-positive one. One set of *S. frugiperda* 21 cells was infected to coexpress λ1Δ28-175 (as a representative of the CLP-positive λ1 deletion mutants), σ2, and λ2, while another set of *S. frugiperda* 21 cells was infected to coexpress both λ1Δ28-175 and λ1Δ2-314λ1 (a CLP-negative mutant) in addition to σ2 and λ2. The two sets of cells were processed in parallel to obtain purified CLPs. The CLPs were then analyzed by SDS-PAGE followed by Coomassie staining (a) or immunoblotting using the polyclonal anti-λ1 serum (b). The bands corresponding to the λ1 deletion mutants are marked at the right.

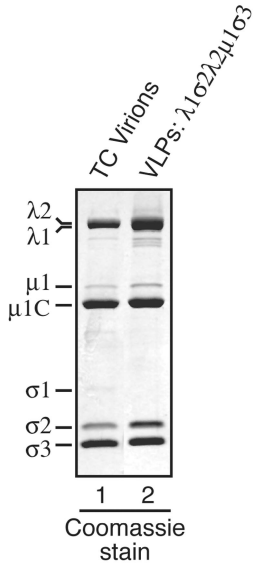

FIG. 9. Coating CLPs with complexes of the major outer-capsid proteins μ1 and σ3 to generate VLPs. (a) An *S. frugiperda* 21 cell lysate containing λ1σ2λ2 CLPs was mixed with a lysate of *T. ni* High Five cells containing complexes of μ1 and σ3 (11, 36). The mixed lysate was incubated and processed to obtain purified particles. These putative VLPs were then analyzed by SDS-PAGE and Coomassie staining (lane 2). Reovirus T1L TC virions (lane 1) were included on the gel to mark the positions of the μ1/μ1C and σ3 proteins as well as to provide a standard for the relative intensities of these bands. The σ1 protein is missing from the VLPs because it was not added in this experiment.

and a single particle band at the expected position for CLPs was observed in the CsCl gradient for each. SDS-PAGE (Fig. 8a) and immunoblotting (Fig. 8b) revealed an additional, λ1-derived band migrating between the λ1Δ28-175 and σ2 bands in the CLPs obtained from the coexpression of λ1Δ2-314 and λ1Δ28-175, but not in the CLPs resulting from the expression of λ1Δ28-175 only (Fig. 8a). Moreover, the position of this extra band was consistent with the size of the λ1Δ2-314 protein (Fig. 7). These findings suggest that the additional band is indeed λ1Δ2-314 and that this mutant had been complemented by λ1Δ28-175 to be assembled into CLPs. Similar evidence for incorporation of the CLP-negative λ1Δ2-259 mutant into CLPs by complementation was obtained in subsequent experiments in which that mutant was coexpressed with full-length λ1, σ2, and λ2 (data not shown). Because λ1Δ2-230 was competent for CLP assembly and because both λ1Δ2-259 and λ1Δ2-314 could be complemented for CLP assembly, we conclude that amino acids in the 231-to-259 region are important for mediating or affecting specific λ1-λ1 or λ1-σ2 interactions that are essential for CLP assembly (see Discussion for further considerations).

λ1σ2λ2, but not λ1σ2, CLPs support in vitro assembly of reovirus outer-capsid proteins μ1 and σ3 to yield VLPs. As a further test of structural and functional similarities between reovirus CLPs and cores, we analyzed whether they can support in vitro assembly of the reovirus outer-capsid proteins μ1 and σ3 (11). An insect cell lysate containing λ1σ2λ2 CLPs (resulting from coexpression of those three proteins) was mixed and incubated with an insect cell lysate containing recombinant μ1-σ3 complexes (resulting from coexpression of those two proteins) (11). The resulting particles were then purified by using the same protocol as that for purification of CLPs. In the CsCl gradient, a predominant upper band accompanied by three or four more minor bands migrating closely beneath (data not shown), resembling the bands seen for the CLPs formed with full-length λ1, was observed (Fig. 2a). For the characterizations in this study, all of these bands were harvested together. The protein compositions of the putative VLP bands were analyzed and compared with those of authentic virions (data not shown) and TC virions (Fig. 9) by SDS-PAGE. Coomassie brilliant blue-stained gels showed that the putative VLPs contain levels of the μ1/μ1C and σ3 proteins similar to those contained by TC virions (Fig. 9), as later confirmed by densitometry (data not shown). Negative-stain EM of the putative λ1σ2λ2μ1σ3 VLPs (Fig. 4d) and TC virions (Fig. 4c) corroborated the gel findings by showing that these two particles have similar sizes and morphologies, including the presence of a thick, double-layered capsid that is clearly distinct from the thinner, single-layered capsid of λ1σ2λ2 CLPs (Fig. 4b). The EM images of λ1σ2λ2μ1σ3 VLPs showed some partially coated particles in addition to more completely coated ones. We believe that the partially coated particles represent intermediates in the process of outer capsid assembly that result from insufficient amounts of the μ1-σ3 complexes that were used in these experiments. In addition, whereas both CLPs and cores have a tendency to aggregate in low-ionic-strength solutions (see the preceding section), the purified VLPs did not show this tendency and remained in

solution at low ionic strength, like virions and TC virions (data not shown). VLPs were also assembled in the same manner from CLPs containing λ1Δ28-175, but in that case a single band was seen in the CsCl gradient, similar to the single band seen with the CLPs assembled with this and other CLP-positive λ1 deletion mutants (see above). From these results, we conclude that the conformations of λ1, σ2, and λ2 on the outer surfaces of CLPs are similar enough to those of authentic cores to support the complete or nearly complete assembly of outer-capsid proteins μ1 and σ3.

We made multiple attempts to form VLPs by coating λ1σ2 CLPs with μ1 and σ3. Since the μ1-σ3 complexes are thought to make contacts with the sides of the λ2 turrets as well as the tops of the σ2 nodules in virions (36), it was conceivable either that the contacts with λ2 are necessary for proper assembly of the μ1-σ3 outer capsid or that the contacts with σ2 are sufficient for this. Evidence from particles formed by reovirus temperature-sensitive mutants previously suggested that the contacts with both λ2 and σ2 are necessary (43, 45). In the present experiments, we obtained no evidence for VLP formation following the attempted coating of λ1σ2 CLPs with μ1 and σ3: particle bands were not seen in the CsCl gradient used as the final step in the purification procedure (data not shown). We conclude that λ2 is necessary for assembly of the μ1-σ3 outer capsid to form VLPs.

DISCUSSION

Generation of CLPs and VLPs from viral proteins expressed in insect cells via recombinant baculoviruses has been previously developed and applied to studies of other members of the *Reoviridae* family including orbiviruses (e.g., bluetongue and Broadhaven viruses) (20, 38, 47) and rotaviruses (15, 33). A powerful aspect of this approach is the capacity to engineer mutations into the different viral structural proteins in order to determine their effects on particle assembly and structure, as well as on at least some functional activities that can be analyzed with these particles (23, 34, 37, 58, 64). In this report, we established the baculovirus-based CLP/VLP system for reoviruses and demonstrated how studies with different subsets and mutant versions of the reovirus structural proteins allow us to address specific questions and hypotheses about particle assembly and structure.

Minimal components for assembly of the core capsid. Our results concur with ones from a previous study indicating that λ1 and σ2 constitute the minimal components for assembly of a stable core capsid that can be purified by established methods (61). We further showed that λ2, μ1, and σ3 can be effectively assembled into particles in this system. Thus, the reovirus proteins that were not included in this study are not strictly required for assembly of these particles. The missing viral proteins comprise the structurally minor core proteins λ3 and μ2, the structurally minor outer-capsid protein σ1, and the nonstructural proteins μNS, σNS, and σ1s. This is not to say that these other viral proteins are dispensable for assembly of reovirus particles within infected cells. Of particular note is that the CLPs and VLPs do not contain the dsRNA genome segments, and thus one or more of these other viral proteins may play a role in genome packaging into particles. Last, the structurally minor proteins λ3, μ2, and σ1 must themselves be incorporated into infectious particles, and preliminary data from our laboratory indicate that all three can indeed be incorporated into CLPs and VLPs by using the recombinant-baculovirus approach (J. Kim and M. L. Nibert, unpublished data). Cellular proteins, yet to be identified, that are sufficiently conserved between insect and mammalian cells may also be required for the particle assembly that we demonstrated in this study.

Our failure to purify CLPs after expression of λ1 in the absence of σ2 or λ2 indicates either (i) that λ1-only CLPs cannot form or (ii) that λ1-only CLPs are fragile and cannot survive the purification procedure. Baculovirus-based expression of rotavirus VP2 (33, 65) or Broadhaven orbivirus VP2 (47), the λ1 equivalents present in 120 copies per core of each virus, is sufficient to give rise to purifiable, single-layer particles. On the other hand, baculovirus-based expression of bluetongue orbivirus VP3, the λ1 and VP2 equivalent present in 120 copies per core of that virus, is not sufficient. Instead, coexpression of VP3 and VP7 (a trimer protein arranged with T=13 [laevo] symmetry in virions and thus most closely analogous to the reovirus μ1 protein) was necessary to generate double-layer particles, which could then be dialyzed at low ionic strength to cause release of VP7 and generation of single-layer particles of VP3 (20, 38). Thus, there are precedents from studies of other *Reoviridae* members that λ1 may contain all the virally encoded signals it needs to assemble into the T=1 shell (rotavirus and Broadhaven virus) or that it may need another, externally bound viral protein to assist in its assembly (bluetongue virus). Although current evidence strongly suggests the latter for λ1, with σ2 being the additional required protein, we are pursuing further experiments to address both these possibilities and to identify probable intermediates in the process of core shell assembly.

Dispensability of the hydrophilic N-terminal arms of λ1 for CLP assembly. The core crystal structure showing the N-terminal arms of λ1.3 wrapped around the threefold axes (Fig. 10a, arms in cyan) clearly suggested that they may be important for tethering together the λ1 decamers within the shell (50). This tethering activity could be required to operate during assembly to bring the decamers together in a productive manner (29) and/or after assembly to stabilize the shell. The results in this study, however, unequivocally demonstrated that the first 230 amino acids of these arms, or almost their full lengths, are not required for assembly of CLPs; for isolation of the CLPs from CsCl gradients; or for additional assembly of the λ2, μ1, and σ3 components of the outer capsid. It is notable that the λ1 equivalents in bluetongue orbivirus (VP3) and group A rotavirus (VP2) appear to contain shorter versions of these N-terminal arms (50 to 100 amino acids) (24, 64), which have been shown not to be required for CLP assembly in the rotavirus case (64). The N-terminal region of rotavirus VP2 is, however, required for incorporating the structurally minor core proteins VP1 and VP3 into CLPs (64). For reoviruses, there is still a question as to what role these N-terminal arms of either the λ1.3 or the λ1.5 subunits may play. One possibility is that in one or both types of λ1 subunits in cores the N-terminal arms may be required for binding the structurally minor core proteins λ3 and μ2. The hydrophilic (positively charged, pI $\approx$ 10 for amino acids 1 to 180 [27]) N-terminal region of λ1, though substantially longer, is also suggestive of

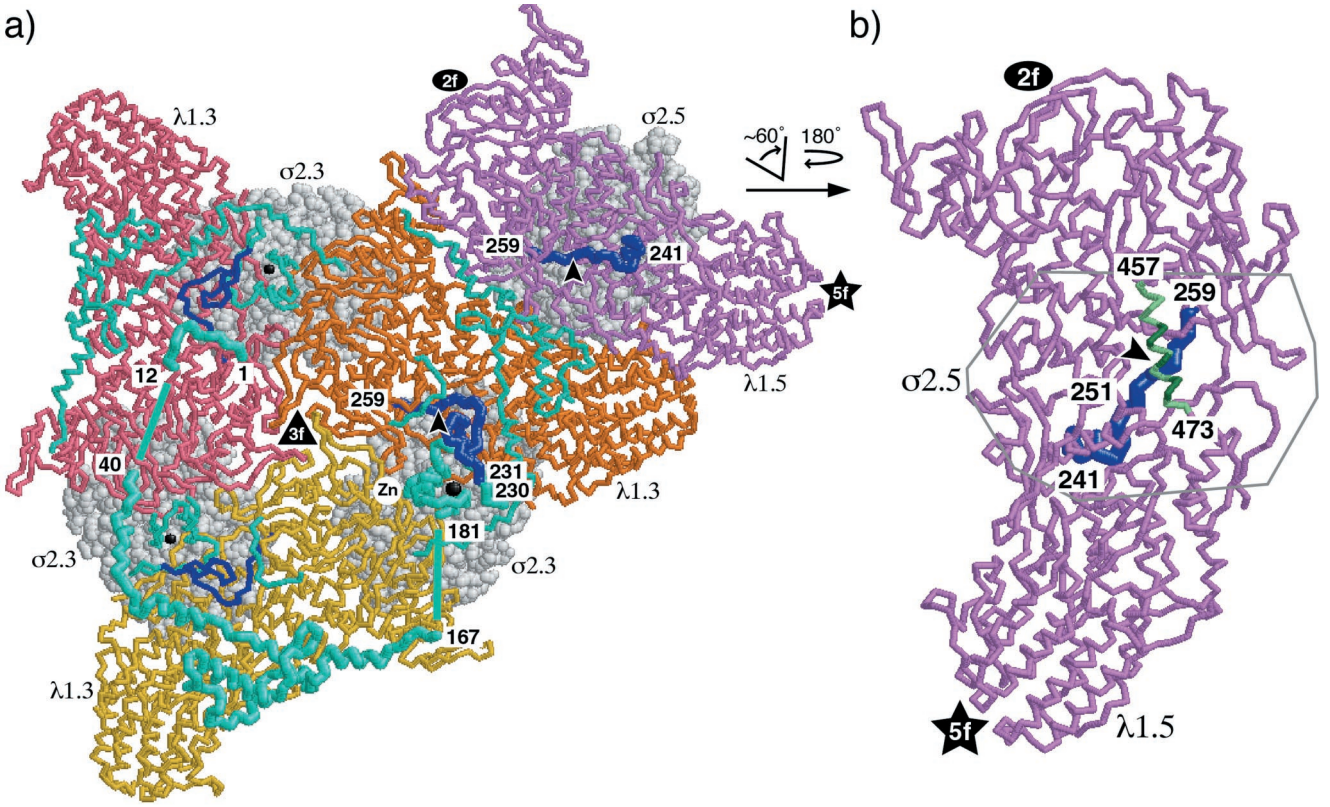

FIG. 10. Views of λ1 and σ2 from the reovirus core crystal structure. Approximate locations of the threefold (▲), twofold (⬬), and fivefold (★) axes are marked. (a) Inside-to-outside view of a portion of the T=1 λ1 shell with accompanying σ2 subunits, centered on a threefold axis of the core (50) (see Fig. 5 for whole-particle surface views that aid in orientation). Three λ1.3 subunits are shown, mostly in pink, orange, or yellow (backbone format). One λ1.5 subunit is also shown, mostly in violet (backbone format). The σ2.3 and σ2.5 subunits that associate with the tops of these λ1 subunits are shown in light gray (space-filling format). Amino acids 1 to 259 of each λ1 subunit (maximum extent of N-terminal sequences that were removed from the deletion mutants in this study) are shown in cyan or blue for emphasis. Amino acids 1 to 240 were not visualized in the core crystal structure of the λ1.5 subunits (50) and are thus not shown in this diagram. In the one λ1.5 subunit pictured, amino acids 241 to 259 are shown in blue as well as in thicker backbone format for greater emphasis. The 251-to-259 region of this subunit adopts an extended conformation and is seen diving into the main body of λ1 (arrowhead) beneath the σ2.5 subunit. Amino acids 1 to 259 of one λ1.3 subunit (the one for which amino acids 260 to 1275 are shown in orange) are shown in thicker backbone format for greater emphasis of that subunit. Amino acids 13 to 39 and 168 to 180 were not visualized in the core crystal structure of the λ1.3 subunits (50), but their proposed locations (50) are shown for the emphasized λ1.3 subunit as straight lines between the flanking visualized regions. In all three λ1.3 subunits pictured, amino acids 1 to 230 are shown in cyan and amino acids 231 to 259 are shown in blue. The 251-to-259 regions of these subunits also adopt extended conformations and can be seen diving into the main body of λ1 (arrowhead for the emphasized subunit) beneath the σ2.3 subunit. The zinc ion in the zinc finger of each λ1.3 subunit is shown as a black ball, which is larger and labeled for the emphasized subunit. (b) The violet λ1.5 subunit from panel a was enlarged and rotated as indicated such that the view of this subunit is now that from outside the core. Amino acids 241 to 259 are shown in blue and in thicker backbone format as in panel a. The arrowhead points to approximately the same position in the λ1.5 subunit as in panel a. The α-helix composed of amino acids 457 to 473, which overlies the 251-to-259 region, is shown in light and dark green. Residues 463, 464, 467, 470, and 471, which make extensive contacts with the base of the overlying σ2.5 subunit, are shown in dark green. Only the outline of the σ2.5 subunit is shown to allow clear views of the underlying λ1.5 subunit.

the RNA-binding, N-terminal domains found in several other viral capsid proteins including those of tomato bushy stunt virus, a tombusvirus, and pariacato virus, a nodavirus (26, 50, 59). Thus, this region of λ1 may also be involved in interactions with the genomic RNA (see below).

Location of λ1 amino acids 231 to 259 in the crystal structure of cores and role of σ2 in CLP assembly. Results from the series of λ1 deletion mutants in this report demonstrated that amino acids 231 to 259 of λ1 play an essential role in CLP formation. In an attempt to understand how these residues may work in assembly, we identified their locations in the reovirus core crystal structure (50). From the view of λ1 (λ1.5 and λ1.3) from inside the particle (Fig. 10a), we can see that residues 241 to 259 of λ1.5 and residues 231 to 259 of λ1.3 are mostly exposed on the inside face of the λ1 shell. (Recall that the first 240 amino acids of λ1.5 are not visible in the crystal structure [50].) These residues are located under the middle part of the body of each respective λ1 subunit and are thus not likely to be involved in interactions between λ1 subunits. Although amino acids 241 to 250 of λ1.5 and 231 to 250 of λ1.3 project from the inside face of the λ1 shell, residues 251 to 259 (Asp-Thr-Pro-Arg-Leu-Val-Thr-Trp-Asp) of both λ1.5 and λ1.3 are partially embedded within the shell in an extended conformation (Fig. 10). This location suggests that λ1 residues 251 to 259 may be important for determining the local conformation of both λ1.5 and λ1.3. Interestingly, residues 251 to 259

in λ1.5 and λ1.3 underlie the respective σ2 monomer that binds atop the λ1 shell in that position (σ2.5 atop λ1.5 and σ2.3 atop λ1.3) (Fig. 10). In neither λ1.5 nor λ1.3, however, do residues 251 to 259 interact directly with σ2. Instead, there is a long α-helix of λ1 (residues 457 to 473) that crosses between residues 251 to 259 and σ2 (not clearly evident in Fig. 10a, but see Fig. 10b). This long α-helix makes several contacts with the bottom of σ2, including contacts by residues 463, 464, 467, 470, and 471 in λ1.5 (Fig. 10b) and residues 466, 470, 471, and 473 in λ1.3. We hypothesize that the deletion of λ1 residues in this 251-to-259 region was the primary determinant of the CLP-negative phenotype of the λ1Δ2-259 deletion mutant because these residues must interact with the α-helix at residues 457 to 473 of λ1 to maintain the proper local conformation of λ1 for it to interact productively with the overlying σ2 monomer. This hypothesis is consistent with the evidence that λ1 and σ2 are the minimal components for core capsid formation, presumably because the σ2 clamps are essential for assembling or stabilizing the λ1 shell by bridging the λ1 subunits within or between decamers (31, 50).

Role for λ2 in assembly of the outer capsid. Previous genetic and biochemical data (29, 44, 45, 54), as well as more recent data from "core-recoating" experiments (11, 12), suggested that assembly of the outer capsid is, or at least can be, uncoupled from assembly of the core. Our present data support this hypothesis by providing evidence that λ1σ2λ2μ1σ3 VLPs can be generated by coating preformed λ1σ2λ2 CLPs with separately preformed μ1-σ3 complexes. The previous data also suggested that the λ2 protein in cores is essential for outer-capsid assembly (29, 45), and our present data support that hypothesis as well by showing that VLPs cannot be generated by addition of μ1-σ3 to λ1σ2 CLPs. Why is λ2 needed for outer-capsid assembly? Don't the μ1 interactions with σ2 (36) suffice to allow the μ1-σ3 lattice to be formed? Two possibilities, which are not mutually exclusive, are (i) that λ2 is required to initiate μ1-σ3 assembly around the turrets and (ii) that the interactions with λ2 are needed to stabilize the μ1-σ3 lattice because the interactions with σ2 are not sufficiently strong. The fact that the λ1σ2 CLP bands disappeared from the CsCl gradient in the coating experiments (data not shown) suggests that μ1-σ3 complexes indeed bound to these particles but did not complete assembly of the outer capsid to allow a discrete particle band to appear in the gradient. The available crystal structures of the λ2 and σ2 proteins in cores (50) and the μ1 protein in μ1-σ3 complexes (36), coupled with the model for how λ2 and μ1-σ3, as well as σ2 and μ1, interact in virions as indicated by a fit of the crystal structures into a cryoEM map of reovirus virions (36), will be useful for designing future experiments to determine the relative roles of λ2 and σ2 in outer-capsid assembly.

CLPs and VLPs with different buoyant densities. Observations in this study that we have yet to explain in full were the presence of different bands of CLPs and VLPs, representing particles of different buoyant densities, that we obtained from the CsCl gradients of the particles prepared to contain the full-length λ1 protein (Fig. 2a). The fact that particles prepared with any versions of λ1 with N-terminal deletions showed only the one, least-dense band (Fig. 2b) suggests that λ1 amino acids in the 2-to-26 range as well as ones in the 28-to-175 range can independently affect this phenotype. Since the hydrophilic N-terminal domain of λ1 has been shown to mediate nucleic acid binding (9, 35), one reasonable possibility is that the different bands reflect incorporation of different amounts of RNA into the particles and that this RNA incorporation is eliminated by the λ1 deletions. Preliminary evidence suggests that the CLPs and VLPs may indeed incorporate a small amount of RNA (J. Kim and M. L. Nibert, unpublished data), but differences among particles containing different λ1 mutants remain to be explored. An opportunity to use the CLP/VLP system to study RNA packaging would be an exciting development.

ACKNOWLEDGMENTS

We are grateful to K. M. Reinisch, Y. Tao, and S. C. Harrison for providing atomic coordinate files for the crystal structure of reovirus cores. Many thanks go also to R. L. Margraf, S. J. Harrison, L. A. Breun, and E. C. Freimont for technical assistance and the other members of our laboratory for helpful discussions.

This work was supported in part by NIH grants R29 AI-39533 and R01 AI-47904 (to M.L.N.) and R01 GM-33050 (to T.S.B.), NSF shared-instrumentation grant BIR-9112921 (to T.S.B.), an instrumentation reinvestment grant from Purdue University to the Purdue Structural Biology faculty, and a USDA Hatch grant through the University of Wisconsin Extension (to M.L.N.).

REFERENCES

1. **Acs, G., H. Klett, M. Schonberg, J. Christman, D. H. Levin, and S. C. Silverstein.** 1971. Mechanism of reovirus double-stranded ribonucleic acid synthesis in vivo and in vitro. J. Virol. **8:**684–689.
2. **Baker, T. S., and R. H. Cheng.** 1996. A model-based approach for determining orientations of biological macromolecules imaged by cryo-electron microscopy. J. Struct. Biol. **116:**120–130.
3. **Baker, T. S., N. H. Olson, and S. D. Fuller.** 1999. Adding the third dimension to virus life cycles: three-dimensional reconstruction of icosahedral viruses from cryo-electron micrographs. Microbiol. Mol. Biol. Rev. **63:**862–922.
4. **Banerjee, A. K., and M. A. Grece.** 1971. An identical 3′-terminal sequence in the ten reovirus genome RNA segments. Biochem. Biophys. Res. Commun. **45:**1518–1525.
5. **Banerjee, A. K., R. Ward, and A. J. Shatkin.** 1971. Cytosine at the 3′-termini of reovirus genome and in vitro mRNA. Nat. New Biol. **232:**114–115.
6. **Bartlett, J. A., and W. K. Joklik.** 1988. The sequence of the reovirus serotype 3 L3 genome segment which encodes the major core protein lambda 1. Virology **167:**31–37.
7. **Bisaillon, M., J. Bergeron, and G. Lemay.** 1997. Characterization of the nucleoside triphosphate phosphohydrolase and helicase activities of the reovirus λ1 protein. J. Biol. Chem. **272:**18298–18303.
8. **Bisaillon, M., and G. Lemay.** 1997. Characterization of the reovirus λ1 protein RNA 5′-triphosphatase activity. J. Biol. Chem. **272:**29954–29957.
9. **Bisaillon, M., and G. Lemay.** 1997. Molecular dissection of the reovirus lambda1 protein nucleic acids binding site. Virus Res. **51:**231–237.
10. **Centonze, V. E., Y. Chen, T. F. Severson, G. G. Borisy, and M. L. Nibert.** 1995. Visualization of individual reovirus particles by low-temperature, high-resolution scanning microscopy. J. Struct. Biol. **115:**215–225.
11. **Chandran, K., S. B. Walker, Y. Chen, C. M. Contreras, L. A. Schiff, T. S. Baker, and M. L. Nibert.** 1999. In vitro recoating of reovirus cores with baculovirus-expressed outer-capsid proteins μ1 and σ3. J. Virol. **73:**3941–3950.
12. **Chandran, K., X. Zhang, N. O. Olson, S. B. Walker, J. D. Chappell, T. S. Dermody, T. S. Baker, and M. L. Nibert.** 2001. Complete in vitro assembly of the reovirus outer capsid produces highly infectious particles suitable for genetic studies of the receptor-binding protein. J. Virol. **75:**5335–5342.
13. **Cleveland, D. R., H. Zarbl, and S. Millward.** 1986. Reovirus guanylyltransferase is L2 gene product lambda 2. J. Virol. **60:**307–311.
14. **Coombs, K. M.** 1998. Stoichiometry of reovirus structural proteins in virus, ISVP, and core particles. Virology **243:**218–228.
15. **Crawford, S. E., M. Labbe, J. Cohen, M. H. Burroughs, Y. J. Zhou, and M. K. Estes.** 1994. Characterization of virus-like particles produced by the expression of rotavirus capsid proteins in insect cells. J. Virol. **68:**5945–5952.
16. **Dermody, T. S., L. A. Schiff, M. L. Nibert, K. M. Coombs, and B. N. Fields.** 1991. The S2 gene nucleotide sequences of prototype strains of the three reovirus serotypes: characterization of reovirus core protein σ2. J. Virol. **65:**5721–5731.
17. **Drayna, D., and B. N. Fields.** 1982. Activation and characterization of the reovirus transcriptase: genetic analysis. J. Virol. **41:**110–118.
18. **Dryden, K. A., D. L. Farsetta, G. Wang, J. M. Keegan, B. N. Fields, T. S.**

Baker, and M. L. Nibert. 1998. Internal structures containing transcriptase-related proteins in top component particles of mammalian orthoreovirus. Virology **245:**33–46.
19. **Dryden, K. A., G. Wang, M. Yeager, M. L. Nibert, K. M. Coombs, D. B. Furlong, B. N. Fields, and T. S. Baker.** 1993. Early steps in reovirus infection are associated with dramatic changes in supramolecular structure and protein conformation: analysis of virions and subviral particles by cryoelectron microscopy and image reconstruction. J. Cell Biol. **122:**1023–1041.
20. **French, T. J., and P. Roy.** 1990. Synthesis of bluetongue virus (BTV) corelike particles by a recombinant baculovirus expressing the two major structural core proteins of BTV. J. Virol. **64:**1530–1536.
21. **Furlong, D. B., M. L. Nibert, and B. N. Fields.** 1988. Sigma 1 protein of mammalian reoviruses extends from the surfaces of viral particles. J. Virol. **62:**246–256.
22. **Furuichi, Y., S. Muthukrishnan, J. Tomasz, and A. J. Shatkin.** 1976. Caps in eukaryotic mRNAs: mechanism of formation of reovirus mRNA 5′-terminal m7GpppGm-C. Prog. Nucleic Acid Res. Mol. Biol. **19:**3–20.
23. **Gilbert, J. M., and H. B. Greenberg.** 1998. Cleavage of rhesus rotavirus VP4 after arginine 247 is essential for rotavirus-like particle-induced fusion from without. J. Virol. **72:**4555–4563.
24. **Grimes, J. M., J. N. Burroughs, P. Gouet, J. M. Diprose, R. Malby, S. Zientara, P. P. Mertens, and D. I. Stuart.** 1998. The atomic structure of the bluetongue virus core. Nature **395:**470–478.
25. **Hager, D. A., and R. R. Burgess.** 1980. Elution of proteins from sodium dodecyl sulfate-polyacrylamide gels, removal of sodium dodecyl sulfate, and renaturation of enzymatic activity: results with sigma subunit of *Escherichia coli* RNA polymerase, wheat germ DNA topoisomerase, and other enzymes. Anal. Biochem. **109:**76–86.
26. **Harrison, S. C.** 1980. Molecular packing of nucleic acids in spherical viruses. Prog. Clin. Biol. Res. **40:**301–310.
27. **Harrison, S. J., D. L. Farsetta, J. Kim, S. Noble, T. J. Broering, and M. L. Nibert.** 1999. Mammalian reovirus L3 gene sequences and evidence for a distinct amino-terminal region of the λ1 protein. Virology **258:**54–64.
28. **Hastings, K. E., and S. Millward.** 1981. Similar sets of terminal oligonucleotides from reovirus double-stranded RNA and viral messenger RNA synthesized in vitro. Can. J. Biochem. **59:**151–157.
29. **Hazelton, P. R., and K. M. Coombs.** 1999. The reovirus mutant *tsA279* L2 gene is associated with generation of a spikeless core particle: implications for capsid assembly. J. Virol. **73:**2298–2308.
30. **Hewat, E. A., T. F. Booth, P. T. Loudon, and P. Roy.** 1992. Three-dimensional reconstruction of baculovirus expressed bluetongue virus core-like particles by cryo-electron microscopy. Virology **189:**10–20.
31. **Hill, C., T. Booth, B. Prasad, J. Grimes, P. Mertens, G. Sutton, and D. Stuart.** 1999. The structure of a cypovirus and the functional organization of dsRNA viruses. Nat. Struct. Biol. **6:**565–568.
32. **Koonin, E. V.** 1993. Computer-assisted identification of a putative methyltransferase domain in NS5 protein of flaviviruses and λ2 protein of reovirus. J. Gen. Virol. **74:**733–740.
33. **Labbe, M., A. Charpilienne, S. E. Crawford, M. K. Estes, and J. Cohen.** 1991. Expression of rotavirus VP2 produces empty corelike particles. J. Virol. **65:**2946–2952.
34. **Lawton, J. A., C. Q. Zeng, S. K. Mukherjee, J. Cohen, M. K. Estes, and B. V. V. Prasad.** 1997. Three-dimensional structural analysis of recombinant rotavirus-like particles with intact and amino-terminal-deleted VP2: implications for the architecture of the VP2 capsid layer. J. Virol. **71:**7353–7360.
35. **Lemay, G., and C. Danis.** 1994. Reovirus λ1 protein: affinity for double-stranded nucleic acids by a small amino-terminal region of the protein independent from the zinc finger motif. J. Gen. Virol. **75:**3261–3266.
36. **Liemann, S., K. Chandran, T. S. Baker, M. L. Nibert, and S. C. Harrison.** 2002. Structure of the reovirus membrane-penetration protein, μ1, in a complex with its protector protein, σ3. Cell **108:**283–295.
37. **Limn, C. K., N. Staeuber, K. Monastyrskaya, P. Gouet, and P. Roy.** 2000. Functional dissection of the major structural protein of bluetongue virus: identification of key residues within VP7 essential for capsid assembly. J. Virol. **74:**8658–8669.
38. **Loudon, P. T., and P. Roy.** 1991. Assembly of five bluetongue virus proteins expressed by recombinant baculoviruses: inclusion of the largest protein VP1 in the core and virus-like proteins. Virology **180:**798–802.
39. **Luongo, C. L., C. M. Contreras, D. L. Farsetta, and M. L. Nibert.** 1998. Binding site for *S*-adenosyl-L-methionine in a central region of mammalian reovirus λ2 protein. Evidence for activities in mRNA cap methylation. J. Biol. Chem. **273:**23773–23780.
40. **Luongo, C. L., K. A. Dryden, D. L. Farsetta, R. L. Margraf, T. F. Severson, N. H. Olson, B. N. Fields, T. S. Baker, and M. L. Nibert.** 1997. Localization of a C-terminal region of λ2 protein in reovirus cores. J. Virol. **71:**8035–8040.
41. **Luongo, C. L., K. M. Reinisch, S. C. Harrison, and M. L. Nibert.** 2000. Identification of the guanylyltransferase region and active site in reovirus mRNA capping protein λ2. J. Biol. Chem. **275:**2804–2810.
42. **Luongo, C. L., X. Zhang, S. B. Walker, Y. Chen, T. J. Broering, D. L. Farsetta, V. D. Bowman, T. S. Baker, and M. L. Nibert.** 2002. Loss of activities for mRNA synthesis accompanies loss of λ2 spikes from reovirus cores: an effect of λ2 on λ1 shell structure. Virology **296:**24–38.
43. **Matsuhisa, T., and W. K. Joklik.** 1974. Temperature-sensitive mutants of reovirus. V. Studies on the nature of the temperature-sensitive lesion of the group C mutant ts447. Virology **60:**380–389.
44. **Morgan, E. M., and H. J. Zweerink.** 1975. Characterization of transcriptase and replicase particles isolated from reovirus-infected cells. Virology **68:**455–466.
45. **Morgan, E. M., and H. J. Zweerink.** 1974. Reovirus morphogenesis. Corelike particles in cells infected at 39 degrees with wild-type reovirus and temperature-sensitive mutants of groups B and G. Virology **59:**556–565.
46. **Morozov, S. Y.** 1989. A possible relationship of reovirus putative RNA polymerase to polymerases of positive-strand RNA viruses. Nucleic Acids Res. **17:**5394.
47. **Moss, S. R., and P. A. Nuttall.** 1994. Subcore- and core-like particles of Broadhaven virus (BRDV), a tick-borne orbivirus, synthesized from baculovirus expressed VP2 and VP7, the major core proteins of BRDV. Virus Res. **32:**401–407.
48. **Noble, S., and M. L. Nibert.** 1997. Characterization of an ATPase activity in reovirus cores and its genetic association with core-shell protein λ1. J. Virol. **71:**2182–2191.
49. **Noble, S., and M. L. Nibert.** 1997. Core protein μ2 is a second determinant of nucleoside triphosphatase activities by reovirus cores. J. Virol. **71:**7728–7735.
50. **Reinisch, K. M., M. L. Nibert, and S. C. Harrison.** 2000. Structure of the reovirus core at 3.6 Å resolution. Nature **404:**960–967.
51. **Schonberg, M., S. C. Silverstein, D. H. Levin, and G. Acs.** 1971. Asynchronous synthesis of the complementary strands of the reovirus genome. Proc. Natl. Acad. Sci. USA **68:**505–508.
52. **Seliger, L. S., K. Zheng, and A. J. Shatkin.** 1987. Complete nucleotide sequence of reovirus L2 gene and deduced amino acid sequence of viral mRNA guanylyltransferase. J. Biol. Chem. **262:**16289–16293.
53. **Shatkin, A. J., and M. Kozak.** 1983. Biochemical aspects of reovirus transcription and translation, p. 79–106. *In* W. K. Joklik (ed.), The *Reoviridae*. Plenum Press, New York, N.Y.
54. **Shing, M., and K. M. Coombs.** 1996. Assembly of the reovirus outer capsid requires μ1/σ3 interactions which are prevented by misfolded σ3 protein in temperature-sensitive mutant tsG453. Virus Res. **46:**19–29.
55. **Skehel, J. J., and W. K. Joklik.** 1969. Studies on the in vitro transcription of reovirus RNA catalyzed by reovirus cores. Virology **39:**822–831.
56. **Smith, R. E., H. J. Zweerink, and W. K. Joklik.** 1969. Polypeptide components of virions, top component and cores of reovirus type 3. Virology **39:**791–810.
57. **Starnes, M. C., and W. K. Joklik.** 1993. Reovirus protein λ3 is a poly(C)-dependent poly(G) polymerase. Virology **193:**356–366.
58. **Tan, B. H., E. Nason, N. Staeuber, W. Jiang, K. Monastryrskaya, and P. Roy.** 2001. RGD tripeptide of bluetongue virus VP7 protein is responsible for core attachment to *Culicoides* cells. J. Virol. **75:**3937–3947.
59. **Tang, L., K. N. Johnson, L. A. Ball, T. Lin, M. Yeager, and J. E. Johnson.** 2001. The structure of pariacato virus reveals a dodecahedral cage of duplex RNA. Nat. Struct. Biol. **8:**77–83.
60. **Virgin, H. W., IV, M. A. Mann, B. N. Fields, and K. L. Tyler.** 1991. Monoclonal antibodies to reovirus reveal structure/function relationships between capsid proteins and genetics of susceptibility to antibody action. J. Virol. **65:**6772–6781.
61. **Xu, P., S. E. Miller, and W. K. Joklik.** 1993. Generation of reovirus core-like particles in cells infected with hybrid vaccinia viruses that express genome segments L1, L2, L3, and S2. Virology **197:**726–731.
62. **Xu, X., S. H. Kang, O. Heidenreich, Q. Li, and M. Nerenberg.** 1996. Rapid PCR method for site-directed mutagenesis on double-stranded plasmid DNA. BioTechniques **20:**44–47.
63. **Yin, P., M. Cheang, and K. M. Coombs.** 1996. The M1 gene is associated with differences in the temperature optimum of the transcriptase activity in reovirus core particles. J. Virol. **70:**1223–1227.
64. **Zeng, C. Q., M. K. Estes, A. Charpilienne, and J. Cohen.** 1998. The N terminus of rotavirus VP2 is necessary for encapsidation of VP1 and VP3. J. Virol. **72:**201–208.
65. **Zeng, C. Q., M. Labbe, J. Cohen, B. V. V. Prasad, D. Chen, R. F. Ramig, and M. K. Estes.** 1994. Characterization of rotavirus VP2 particles. Virology **201:**55–65.
66. **Zeng, C. Q., M. J. Wentz, J. Cohen, M. K. Estes, and R. F. Ramig.** 1996. Characterization and replicase activity of double-layered and single-layered rotavirus-like particles expressed from baculovirus recombinants. J. Virol. **70:**2736–2742.